

1  
2  
3  
4  
5  
6  
7  
8  
9  
10  
11  
12  
13  
14  
15  
16  
17  
18  
19  
20  
21  
22  
23  
24  
25  
26  
27

**Multinucleotide mutations cause false inferences of lineage-specific positive selection**

Aarti Venkat<sup>1</sup>, Matthew W. Hahn<sup>2</sup>, Joseph W. Thornton<sup>\*1,3</sup>

(1) Department of Human Genetics, University of Chicago, Chicago IL 60637, USA

(2) Department of Biology and Department of Computer Science, Indiana University,  
Bloomington IN 47405, USA

(3) Department of Ecology & Evolution, University of Chicago, Chicago IL 60637, USA

\*Correspondence: Joseph Thornton, [joet1@uchicago.edu](mailto:joet1@uchicago.edu)

Keywords: adaptation, adaptive evolution, branch-site test, codon models, transversions

28  
29  
30  
31  
32  
33  
34  
35  
36  
37  
38  
39  
40  
41  
42  
43  
44  
45  
46  
47  
48  
49  
50  
51  
52  
53

**ABSTRACT**

Phylogenetic tests of adaptive evolution, which infer positive selection from an excess of nonsynonymous changes, assume that nucleotide substitutions occur singly and independently. But recent research has shown that multiple errors at adjacent sites often occur in single events during DNA replication. These multinucleotide mutations (MNM) are overwhelmingly likely to be nonsynonymous. We therefore evaluated whether phylogenetic tests of adaptive evolution, such as the widely used branch-site test, might misinterpret sequence patterns produced by MNMs as false support for positive selection. We explored two genome-wide datasets comprising thousands of coding alignments – one from mammals and one from flies – and found that codons with multiple differences (CMDs) account for virtually all the support for lineage-specific positive selection inferred by the branch-site test. Simulations under genome-wide, empirically derived conditions without positive selection show that realistic rates of MNMs cause a strong and systematic bias in the branch-site and related tests; the bias is sufficient to produce false positive inferences approximately as often as the branch-site test infers positive selection from the empirical data. Our analysis indicates that genes may often be inferred to be under positive selection simply because they stochastically accumulated one or a few MNMs. Because these tests do not reliably distinguish sequence patterns produced by authentic positive selection from those caused by neutral fixation of MNMs, many published inferences of adaptive evolution using these techniques may therefore be artifacts of model violation caused by unincorporated neutral mutational processes. We develop an alternative model that incorporates MNMs and may be helpful in reducing this bias.

## 54 INTRODUCTION

55

56 Identifying genes that evolved under the influence of positive natural selection is a  
57 central goal in molecular evolutionary biology. During recent decades, likelihood-based  
58 phylogenetic methods have been developed to identify gene sequences that retain putative  
59 signatures of past positive selection<sup>1-10</sup>. Perhaps the most widely used of these is the branch-site  
60 test (BST) of episodic selection, which allows positive selection to affect only some codons on  
61 one or a few specified branches of a phylogeny, and therefore has relatively high power  
62 compared to methods that detect selection across an entire sequence or an entire phylogenetic  
63 tree<sup>5,6,11</sup>. The BST has been the basis for published claims of lineage-specific adaptive  
64 evolution in many thousands of individual genes<sup>12-16</sup>.

65 The BST and related methods use a likelihood ratio test to compare how well two  
66 mixture models of sequence evolution on a phylogeny fit an alignment of coding sequence data.  
67 The null model constrains all codons to evolve with rates of nonsynonymous substitution ( $d_N$ )  
68 less than or equal to the rate of synonymous substitution ( $d_S$ ), as expected under purifying  
69 selection and drift. In the positive selection model, some sites are allowed to have  $d_N > d_S$  on a  
70 branch or branches of interest. If the increase in likelihood of this model given the data is greater  
71 than expected due to chance alone, the null model is rejected and adaptive evolution is inferred.  
72 The BST has been shown to be conservative, with a low rate of false positive inferences, when  
73 sequences are generated under an evolutionary process corresponding to the null model<sup>6,11</sup>. It is  
74 widely appreciated that likelihood ratio tests can become biased if the underlying probabilistic  
75 model is incorrect<sup>17</sup>. The effect on the BST of a few forms of model violation—such as an  
76 unequal distribution of selective effects among sites, positive selection on non-foreground  
77 lineages, high sequence divergence, and non-allelic gene conversion—have been previously  
78 studied<sup>18-22</sup> and the test has been found to be reasonably robust to most but not all forms of  
79 violation examined<sup>6,23,24</sup>.

80 Recent research in molecular genetics and genomics suggests a potentially important  
81 phenomenon that has not been incorporated into models used in tests of positive selection: the  
82 propensity of DNA polymerases to produce mutations at neighboring sites. All implementations  
83 of the BST and other likelihood-based tests of adaptive evolution use models in which mutations  
84 occur only at individual nucleotide sites and are fixed singly and independently. Codons with  
85 multiple differences between them can be interconverted only by serial single-nucleotide

86 substitutions, the probability of which is the product of the probabilities of each independent  
87 event. Recent molecular studies have shown, however, that mutations affecting adjacent  
88 nucleotide sites often occur during replication, apparently because certain DNA microstructures  
89 recruit error-prone polymerases that lack proofreading activity and therefore make multiple  
90 errors close together<sup>25–33</sup>. Consistent with these mechanisms, genetic studies of human trios and  
91 mutation-accumulation experiments in laboratory organisms indicate that *de novo* mutations  
92 occur in tandem or at nearby sites more frequently than expected if each occurred independently  
93<sup>25,32–36</sup>, and these multinucleotide mutations (MNMs) are enriched in transversions<sup>35,37,39</sup>. The  
94 precise frequency at which MNMs occur is difficult to estimate, but a recent compilation of  
95 genetic studies in humans concluded that about 0.4% of mutations, polymorphisms, and  
96 substitutions are at directly adjacent sites (counting each tandem pair as one event)<sup>34</sup>. In  
97 *Drosophila melanogaster* genomes, analysis of rare polymorphisms and mutation-accumulation  
98 experiments estimated that 1.3% of all mutations are at adjacent sites<sup>38</sup>. Although the methods  
99 and data sources in these studies differ, these findings suggest that tandem MNMs probably  
100 account for on the order of 1% of mutational events.

101 We hypothesized that these mutational processes might lead to false signatures of  
102 positive selection in the BST. Because of the structure of the genetic code, virtually all MNMs  
103 in coding sequences are nonsynonymous, and most would comprise multiple nonsynonymous  
104 nucleotide changes if they were to occur by single nucleotide steps (**Supplementary Table 1**).  
105 The enrichment of transversions in MNMs further increases the propensity for MNMs to produce  
106 nonsynonymous changes, because transversions are more likely than transitions to be  
107 nonsynonymous. MNMs are therefore likely to produce codons with multiple differences  
108 (CMDs) that contain an apparent excess of nonsynonymous substitutions. When these CMDs are  
109 assessed using a method that treats all substitutions as independent events, a model that allows  
110  $d_N$  to exceed  $d_S$  at some sites may have a higher likelihood than one that restricts  $d_N/d_S$  to values  
111  $\leq 1$ . Further, the assumption that all mutations have the same transversion-transition rate might  
112 exacerbate the tendency to misinterpret MNM-produced nonsynonymous changes as evidence  
113 for positive selection. Of course, CMDs can also be driven to fixation by positive selection<sup>11,40–</sup>  
114<sup>42</sup>—and the same is true of transversion-rich substitutions—but these considerations suggest that  
115 failing to incorporate MNMs in likelihood models might make tests of adaptive evolution  
116 susceptible to false positive inferences. The BST and other lineage-specific tests might be

117 particularly sensitive to this problem because they seek signatures of positive selection acting on  
118 small numbers of codons on one or a few specified branches of the tree <sup>43</sup>. Simulation studies  
119 suggest that MNMs may elevate false positive rates in some selection tests <sup>44</sup>, but there has been  
120 no comprehensive analysis of the effect of MNMs, particularly on the branch-site test or under  
121 realistic, genome-scale conditions.

122

## 123 **RESULTS**

124

125 To understand the effect of MNMs on the accuracy of the branch-site test, we analyzed in  
126 detail two previously published genome-wide datasets, which represent classic examples of the  
127 application of the test <sup>13,15,45</sup>. The mammalian dataset consists of coding sequences of 16,541  
128 genes from six eutherian mammals; we retained for analysis only the 6,868 genes with complete  
129 species coverage. The fly dataset consists of 8,564 genes from six species in the melanogaster  
130 subgroup clade, all of which had complete coverage (**Supplementary Fig. 1**). The fly genes  
131 have higher sequence divergence than those in the mammalian dataset, allowing us to examine  
132 the performance of the BST under different evolutionary conditions.

133 We used the classic BST to identify genes putatively under positive selection ( $P < 0.05$ ) on  
134 the human lineage in the mammalian dataset and on each of the six terminal lineages in flies. 82  
135 genes in humans and 3,938 in flies yielded significant tests (**Supplementary Table 2**). To  
136 facilitate robust further analysis of CMDs, we filtered out genes in which CMDs occur at sites  
137 with indels or in which the ancestral states of CMDs are reconstructed differently between the  
138 null and positive selection models; we also applied a multiple testing correction ( $FDR < 0.20$ ). In  
139 flies, 443 genes were retained after these steps. Thirty human genes passed the CMD alignment  
140 and reconstruction filter, but none met the FDR threshold, consistent with previous analyses of  
141 these data; <sup>15</sup> nevertheless, we included the 30 initially significant human genes because this  
142 lineage is the object of intense interest and because its short length contrasts with the fly  
143 branches. These two groups constitute the “BST-significant” sets of genes in flies and humans.

144

## 145 **CMDs provide virtually all support for positive selection**

146 We sought to determine how much of the evidence for positive selection comes from  
147 CMDs. We first observed that CMDs were dramatically enriched in BST-significant genes  
148 compared to non-BST-significant genes (**Fig. 1a**). In humans, BST-significant genes contain  
149 one CMD on average, while BST-nonsignificant genes contain none (**Supplementary Fig. 2**).  
150 The pattern is similar but less extreme in flies, with the average number of CMDs per BST-  
151 significant gene greater than that in non-significant genes (**Supplementary Fig. 2**). When  
152 CMD-containing codons are excluded from the alignments, the vast majority of genes that were  
153 BST-significant lose their signature of selection in both datasets (**Fig. 1b**).

154 We next calculated the fraction of statistical support for positive selection that comes  
155 from CMDs. The total support for positive selection in an alignment is defined as the difference  
156 between the log-likelihood of the positive selection model and that of the null model, summed  
157 across all codons in the alignment. The fraction of support from CMDs is the support from  
158 CMD-containing codons divided by the total support across the entire alignment. CMDs account  
159 for >95% of the support for positive selection in virtually all BST-significant genes in both  
160 datasets; in about 70% of genes, CMDs provide all the support (**Fig. 1c**).

161 Finally, we examined the BST's *a posteriori* identification of sites under positive  
162 selection. We found that CMDs were far more likely to be classified as positively selected than  
163 non-CMDs. Among genes that were BST-significant on the human lineage, every CMD was  
164 inferred to be under positive selection using a Bayes Empirical Bayes posterior probability (PP)  
165 cutoff > 0.5. Using a more stringent cutoff of PP>0.9, 66 percent of CMDs were classified as  
166 positively selected, compared to 0.07% of non-CMDs. In the fly dataset, CMDs accounted for  
167 90% of codons with BEB>0.9, although they represent less than 1% of all codons (**Fig. 1d**).

168 CMDs are therefore the primary drivers of the signature of selection identified in the  
169 BST. A single CMD provides sufficient statistical support to yield a signature of positive  
170 selection on the human lineage, and only a few CMDs in a gene are enough to do the same in  
171 flies.

## 173 **Incorporating MNMs eliminates the signature of positive selection in many genes**

174 CMDs might be enriched in BST-positive genes because of an MNM-induced bias or  
175 because they were fixed by positive selection. To incorporate both neutral and selection-driven

176 fixation of MNMs into a BST framework, we developed a codon model in which double-  
177 nucleotide changes are allowed, with the parameter  $\delta$  serving as a multiplier that modifies the  
178 rate of each double-nucleotide substitution relative to single-nucleotide substitutions. We  
179 implemented a version of the BST (BS+MNM) that is identical to the classic version, except that  
180 both the null and positive selection models allow MNMs. Simulations under conditions derived  
181 from a sample of genes in the mammalian dataset show that the method estimates the parameters  
182 used to generate the sequences with reasonable accuracy (**Supplementary Fig. 3**).

183 We first fit the BS+MNM null model to all alignments in the mammalian and fly  
184 datasets. The average estimate of  $\delta$  across all genes was 0.026 in mammals and 0.062 in flies,  
185 with  $\delta$  in both cases about twice as high in the subset of BST-significant genes as in BST-  
186 nonsignificant genes (**Fig. 2a**). Using a likelihood-ratio test, we found significant support for the  
187 BS+MNM null model (compared to the classic BST null model) in 22% of human genes and  
188 >50% of fly genes (**Supplementary Table 3**); simulations without MNMs showed that this  
189 comparison has a very low false-positive rate (**Supplementary Table 4**).

190 We then used this BS+MNM test to evaluate the empirical sequences for positive  
191 selection. We found that 96% of the BST-significant genes on the human lineage lost  
192 significance in the BS+MNM test (**Figs. 2b, Supplementary Table 5**). In flies, 38% of the  
193 BST-significant genes lost significance; a substantial fraction of those that retained significance  
194 were enriched in triple substitutions, a process not accounted for in our model (**Figs. 2b,**  
195 **Supplementary Table 5**).

196

### 197 **MNMs cause false positive inferences on a genome-wide scale**

198 That the BS+MNM test eliminates the signature of positive selection from many genes  
199 could have several causes, including: 1) the more complex BS+MNM model may have reduced  
200 power to identify authentic positive selection compared to the BST, 2) incorporating MNMs may  
201 ameliorate a bias towards false positive inference in the classic BST that is caused by MNMs,  
202 and 3) the additional  $\delta$  parameter in the BS+MNM test may allow it to incorporate other forms of  
203 sequence complexity, potentially ameliorating a bias caused by other model violations.

204 We addressed these possibilities in two ways. First, we performed power analyses of the  
205 BS+MNM test using simulations in which positive selection is present in the generating model.  
206 We simulated sequence data on the mammalian and fly phylogenies using genome-wide

207 averages for all parameters of the BST positive selection model, but we varied the strength of  
208 positive selection ( $\omega_2$ ) and the proportion of sites under positive selection. We then applied the  
209 BS+MNM test to these data and found that it can reliably detect strong positive selection ( $\omega_2 >$   
210 20) when it affects more than 10% of sites in a typical gene, or moderate positive selection ( $10 <$   
211  $\omega_2 < 20$ ) that affects a larger fraction of sites (**Supplementary Fig. 4a**). Under parameters  
212 derived from both datasets, the test's power is similar to that of the classic BST, with slight  
213 reductions under only a few conditions on the fly lineage. Thus, although some genes may have  
214 lost their signature of selection because of reduced power in the BS+MNM test, it appears  
215 unlikely that a difference in power is the primary cause of the dramatic reduction in the number  
216 of positive results when the test is used.

217         Second, we used simulations under null conditions to directly evaluate the frequency of  
218 false positive inferences by the classic BST when sequences are generated with realistic rates of  
219 multinucleotide mutation. For every gene in the mammalian and fly datasets, we simulated  
220 sequence evolution under the null BS+MNM model without positive selection using parameters  
221 derived from the alignments, including  $\delta$ . These parameters generate sequences with an  
222 observed frequency of tandem substitutions of 1.6% in humans and 3.2% in the *D. melanogaster*  
223 lineage in flies, similar to or slightly higher than the observed frequencies in the empirical  
224 datasets (1.3% and 1.6%, respectively), presumably because the BS+MNM model captures some  
225 but not all aspects of real sequence evolution (**Supplemental Table 6**)<sup>34, 38</sup>.

226         We then analyzed these positive-selection-free simulated data using the classic BST. In  
227 both humans and flies, the number of genes with significant results—all of which are false  
228 positive inferences—was greater than the number of genes that the BST had concluded were  
229 under positive selection using the empirical data (**Fig. 3a**). In flies, almost 9 percent of tests  
230 were false positives ( $P < 0.05$ ), despite the conservative approach the method uses to calculate P-  
231 values<sup>6,11</sup>, compared to just 1 percent under control simulations without MNMs. Further, more  
232 than 1,700 of these false positive tests survived FDR adjustment, compared to just 4 in the  
233 control simulations (**Supplementary Table 2**). In humans, the fraction of false positive  
234 inferences is lower, consistent with the test's reduced power in this dataset, but still about three  
235 times greater than in the control simulations.

236         These false inferences are caused primarily by MNM-induced bias, because simulating  
237 data under identical control conditions without MNMs ( $\delta = 0$ ) produced few positive tests. All



238 other parameters were identical between the generating model and analysis models, so other  
239 forms of model violation do not contribute to the bias observed in the simulation experiments.  
240 Taken together, these findings indicate that MNMs under realistic evolutionary conditions  
241 produce a strong and widespread bias in the BST toward false inferences of positive selection.  
242 This bias is strong enough to cause the BST to make false inferences of positive selection at  
243 about the same rate as it infers selection in the real genomes of humans and flies. In the  
244 simulations, every positive result is false; in the tests of real sequences, the fraction of positive  
245 results that are true is unknown.

246

### 247 **Systematic bias caused by chance MNMs in longer genes**

248 We next sought to identify the causal factors that determine whether a gene yields a false  
249 positive result in the BST because of MNM-induced bias. Most genes are only several hundred  
250 codons long, and only a few percent of mutations are MNMs, so on phylogenetic branches of  
251 short to moderate length many genes will contain no CMDs caused by multinucleotide  
252 mutations. The hypothesis that neutral fixation of MNMs contributes to inferences of positive  
253 selection in the BST predicts that a gene's propensity to produce a BST-significant result should  
254 depend on factors that increase the probability it will contain one or more fixed MNMs by  
255 chance, including its length and the gene-specific rate at which MNMs occur within it.

256 We first tested for an effect of gene length on the results of the branch-site test. As  
257 predicted, we observed that BST-significant empirical genes were on average 100 and 16 codons  
258 longer than non-significant genes in the human and fly empirical datasets, respectively (**Fig. 3b**).  
259 The relationship between length and propensity to yield a BST positive result could arise because  
260 genes that present a larger "target" are more likely to undergo MNMs than shorter genes;  
261 alternatively, longer genes, by including more sites for analysis, might increase the power of the  
262 BST to detect authentic positive selection. However, in genome-wide simulations under the null  
263 model with no positive selection (but with  $\delta > 0$ ), genes with false positive BSTs are longer than  
264 the non-significant genes by an average of 26 and 31 codons using the human and fly  
265 parameters, respectively (**Supplementary Fig. 5**). This result cannot be attributed to increased  
266 power to detect true positive selection and supports the conclusion that mutational target size  
267 contributes to a gene's propensity to manifest MNM-induced bias by chance alone.

268 To directly test the causal relationship between sequence length and false-positive bias in

269 the BST, we simulated sequence evolution at increasing sequence lengths, using evolutionary  
270 parameters derived from each of the BST-significant genes in the mammalian and fly datasets.  
271 For each gene's parameters, we simulated 50 replicate alignments under the BS+MNM null  
272 model and then analyzed them using the classic BST (**Supplementary Fig. 6a**). The false  
273 positive rate for any gene's simulations is defined as the fraction of replicates with a significant  
274 LRT in the classic BST, using a P-value cutoff of 0.05. When sequences 5,000 codons long  
275 were simulated, 96% of BST-significant genes had an unacceptable FPR ( $>0.05$ ), with a median  
276 FPR of 0.39: increasing sequence length to 10,000 codons exacerbated the bias, with 100% of  
277 genes yielding an unacceptable FPR and a median FPR of 0.56 (**Fig. 3c**). In flies, a similar  
278 pattern was evident, and the false positive rates were even higher (median FPR=0.74 and 0.90 at  
279 5,000 and 10,000 codons, respectively). Control simulations under identical conditions but with  
280  $\delta=0$  led to very low FPRs (median 0.02 to 0.03 in both datasets), even with very long sequences  
281 (grey dots in **Fig. 3c**). A similar systematic and length-dependent bias also resulted when  
282 sequences were simulated under gene-specific conditions, but with  $\delta$  fixed to its average across  
283 the thousands of BST-nonsignificant genes in each dataset (**Supplementary Fig. 6b**). Although  
284 the sequence lengths tested are longer than most real genes, these experiments directly establish  
285 that a gene's probability of returning a significant BST result in the absence of positive selection  
286 is directly related to the target size it presents for chance fixation of MNMs.

287 We next evaluated whether the gene-specific rate of multinucleotide mutation affects a  
288 gene's propensity to yield a positive result in the BST. As predicted, we observed that BST-  
289 significant genes in the empirical datasets had higher estimated  $\delta$  than nonsignificant genes (**Fig.**  
290 **2a**). Genes producing false positive results in the genome-wide null simulations under empirical  
291 conditions also tended to have higher  $\delta$  (**Fig 3d**); this result that cannot be attributed to the  
292 possibility that  $\delta$  might be fitting CMDs fixed by positive selection, because positive selection  
293 was absent from the generating model.

294 To directly test the effect of the neutral MNM substitution rate on the BST, we simulated  
295 sequences 5,000 codons long under the null BS+MNM model, with a variable  $\delta$  and all other  
296 parameters fixed to their averages across all genes. We found that increasing  $\delta$  led to a  
297 monotonic increase in the frequency of false positive inferences. The FPR was  $>0.05$  when  $\delta$   
298 was only 0.001 and 0.013 on the human and fly lineages, respectively. When  $\delta$  was equal to its  
299 genome-wide average (0.026 and 0.062 in mammals and flies), false positive inferences occurred

300 at rates of 22 and 17 percent, respectively (**Fig. 3e**). As  $\delta$  increased, so too did the inferred value  
301 of the parameter  $\omega_2$ , which represents the inferred intensity of positive selection in the model  
302 (**Fig. 3f**).

303 Typical evolutionary conditions are therefore sufficient to cause a strong and systemic  
304 bias in the BST. MNMs are rare, however, so longer genes and those with higher rates of  
305 multinucleotide mutation are more likely to undergo this process and manifest the bias. This  
306 view is further supported by the fact that fewer genes are BST-positive on the human branch –  
307 which is so short that substitutions of any type are rare, and MNMs even more so – than on the  
308 fly phylogeny, where branches are longer, more CMDs are apparent, and hundreds of genes have  
309 BST signatures of selection. Taken together, these findings suggest that although some genes  
310 with BST-significant results in empirical datasets could have evolved adaptively, many may  
311 simply be those that happened to fix multinucleotide substitutions by chance alone.

312

### 313 **Transversion-enrichment in CMDs exacerbates bias in the branch-site test**

314 MNMs tend to produce more transversions than classical single-site mutational  
315 processes, so if CMDs are produced by MNMs, they should be transversion-rich<sup>35,37,39</sup>. As  
316 predicted, we found that transversion:transition ratio is elevated in CMDs relative to that in non-  
317 CMDs by factors of three and two in mammals and flies, respectively (**Fig. 4a**). In the subset of  
318 BST-significant genes, CMDs have an even more elevated transversion:transition ratio, as  
319 expected if transversion-rich MNMs bias the test (**Fig. 4a**). These data are consistent with the  
320 hypothesis that a transversion-rich MNM process produced many of the CMDs in BST-  
321 significant genes, but it is also possible that positive selection could have enriched for  
322 transversions.

323 To test whether transversion-enrichment in MNMs exacerbates the BST's bias, we  
324 developed an elaboration of the BS+MNM model in which an additional parameter allows  
325 MNMs to have a different transversion:transition rate ratio ( $\kappa_2$ ) than single-site substitutions do  
326 ( $\kappa_1$ ). We estimated the maximum likelihood estimates of the model's parameters for every gene  
327 in the mammalian and fly datasets and simulated sequences using genome-wide median values  
328 for all model parameters and branch lengths, except for  $\kappa_2$ , which we varied. Sequences 10,000  
329 codons long were used, because simulating shorter sequences resulted in a high variance in the  
330 realized transversion:transition ratio. We analyzed these data using the classic BST and

331 calculated the fraction of replicates in which positive selection was inferred. We found that  
332 increasing  $\kappa_2$  caused a rapid and monotonic increase in the false positive rate, indicating that  
333 transversion enrichment in MNMs exacerbates the test's bias. The effect is strong: when  $\kappa_2/\kappa_1$  is  
334 increased from 1 to 2, the FPR approximately doubles (**Fig. 4b**). Thus, realistic rates of MNM  
335 generation and transversion-enrichment together cause an even stronger bias in the BST than  
336 MNMs alone. This result cannot be accounted for by positive selection driving fixation of  
337 transversions, because no positive selection was present in the simulations.

338

### 339 **MNMs affect a newer test of positive selection**

340 In recent years, newer likelihood-based methods have been introduced to test for episodic  
341 site-specific positive selection<sup>2,3,7</sup>. All these methods are based on models of sequence  
342 evolution that, like the BST, do not allow MNMs but instead model CMDs as the result of serial  
343 site-specific substitutions. We therefore hypothesized that these methods might also be biased  
344 by MNMs. We chose a more recent method, BUSTED<sup>2</sup>, which was developed primarily to test  
345 for episodic site-specific selection events across an entire tree. We tested its performance on  
346 alignments 5,000 codons long that were simulated using the BS+MNM null model and  
347 parameters estimated from the BST-significant gene alignments in humans and flies. To test for  
348 MNM-induced bias, we compared results when  $\delta$  was assigned to three different values: zero, its  
349 average across all alignments in the mammalian or fly datasets, or its gene-specific value in each  
350 of the BST-significant genes (**Supplementary Fig. 6a**).

351 We found that BUSTED was also sensitive to MNM-induced bias. When  $\delta=0$ , virtually  
352 no genes' parameters led to frequent false positive inferences, with a median FPR  $<0.03$  across  
353 genes (**Fig. 5**). But when  $\delta$  was assigned to its empirically estimated gene-specific value, the  
354 parameters from every gene in humans and the majority in flies yielded false positive rates  
355  $>0.05$ , with median FPRs of 0.29 and 0.5, respectively (**Fig. 5**). Frequent false positive  
356 inferences were evident when sequences were simulated using genome-wide average estimates  
357 of  $\delta$ , as well.

358

### 359 **CMDs that invoke multiple nonsynonymous steps drive the signature of positive selection**

360 Finally, we sought further insight into the reasons why CMDs yield a false signature of  
361 positive selection in the BST and related tests. In standard models of codon evolution, CMDs

362 are interpreted as the result of two or more serial independent substitutions, even though they can  
363 be produced by MNMs in a single mutational event. We hypothesized that CMDs that imply  
364 multiple nonsynonymous nucleotide substitutions under these models would provide the  
365 strongest support for the positive selection model. We therefore classified CMDs in the  
366 empirical datasets by the minimum number of nonsynonymous single-nucleotide substitutions  
367 required from the ancestral to derived codon state under standard codon models. As predicted,  
368 we found that CMDs that imply more than one nonsynonymous step are dramatically enriched in  
369 BST-significant genes (**Fig 6a**).

370 We also examined the statistical support provided by different kinds of CMDs. As the  
371 number of nonsynonymous steps increased, the statistical support provided for the positive  
372 selection model also increased (**Fig. 6b**). CMDs that imply one nonsynonymous and one  
373 synonymous step typically provide weak to moderate support for the positive selection model,  
374 but CMDs that imply two nonsynonymous steps provide very strong support. In many cases, a  
375 single CMD in this latter category is sufficient to yield a statistically significant signature of  
376 positive selection.

377

## 378 **DISCUSSION**

379

380 Our results demonstrate that the branch-site test suffers from a strong and systematic bias  
381 toward false positive inferences. This bias is caused by a mismatch between the method's  
382 underlying codon model of evolution – which assumes that a codon with multiple differences can  
383 be produced only by two or more independent substitution events – and the recently discovered  
384 phenomenon of multinucleotide mutation, which produces such codons in a single event.  
385 Because of the structure of the genetic code and the high transversion rates that characterize  
386 MNMs, most codons produced by this mechanism cause more than one nonsynonymous single-  
387 nucleotide change. Confronted with this kind of codon data, the likelihood calculated by the  
388 BST is determined by the product of the probabilities of the individual mutations. Under the null  
389 model, the probability of such compound events is extremely small, but it can increase  
390 dramatically when  $d_N/d_S$  exceeds one, as the positive selection model allows. This increase in  
391 likelihood afforded by the positive selection model is much greater than it would be if the  
392 substitution were interpreted as the result of a single multinucleotide event. Indeed, our results

393 show that a single codon comprising two nonsynonymous substitutions is often sufficient to  
394 yield a statistically significant signature of positive selection in the BST for an entire gene.

395 As a result, CMDs are the primary drivers of positive results by the BST. Virtually all  
396 statistical support for positive selection in real alignments comes from CMD-containing sites;  
397 removing them from the alignment or incorporating MNMs into the BST's model eliminates the  
398 signature of selection from the majority of genes. CMDs can be produced by either positive  
399 selection or by neutral evolution under multinucleotide mutation. In the former case, the BST  
400 will be correct; however, the test cannot reliably distinguish CMDs that represent authentic  
401 evidence of positive selection from those caused by MNM-induced bias.

402 The bias is strong and pervasive under realistic conditions. Indeed, when sequences were  
403 simulated under the null model using parameters estimated from the fly and mammalian datasets,  
404 the number of genes with false positive BSTs was approximately the same as the number of  
405 positive BST results when the empirical data were analyzed. There is therefore no excess of  
406 BST-positive results in these genomes beyond that potentially attributable to MNM-induced bias.  
407 Worse, these null simulations did not include the elevated transversion rate that characterizes  
408 MNMs, which exacerbates the test's bias. Taken together, these results suggest the possibility  
409 that MNM-induced bias could explain many of the BST's inferences of positive selection in  
410 these datasets.

411 Are our findings from these datasets generalizable? MNMs appear to be a property of all  
412 eukaryotic replication processes, and the MNM rates that we observed in mammals and flies are  
413 in the same range as those previously identified in genetic and molecular studies in a variety of  
414 eukaryotic species<sup>25,34,38</sup>. Both datasets comprise a small number of taxa, but the BST seeks  
415 evidence of selection on individual branches, so it seems unlikely that larger trees will somehow  
416 inoculate the test against MNM-induced bias. We observed strong bias on lineages with  
417 divergence levels ranging from very low (on the human terminal branch) to moderate (the fly  
418 branches), so this problem does not appear to be unique to highly diverged sequences or  
419 phylogenies with long branches. We must therefore consider the possibility that many of the  
420 thousands of previously published reports of positive selection based on the BST could simply be  
421 the ones that happened by chance to neutrally fix one or more multinucleotide mutations.

422 We do not contend that the BST is always wrong or that molecular adaptive evolution  
423 does not occur. The existence of a bias, even a strong one, towards false positive inferences does

424 not mean that all positive inferences are false: some of the CMDs in BST-significant genes may  
425 have evolved because of authentic positive selection, either by repeated substitution of single  
426 nucleotides in a codon or selection on MNMs. But because the BST test cannot distinguish the  
427 kinds of sequence data produced by positive selection from those produced by neutral evolution  
428 of MNMs, it does not provide reliable evidence that a gene evolved adaptively; nor does it  
429 provide a reliable estimate of the fraction of genes in a large set that evolved under positive  
430 selection. There are numerous cases of strongly supported adaptive evolution, such as those  
431 involving host-parasite and intracellular genetic conflicts, that have produced sequence  
432 signatures of positive selection in the BST and related tests that are likely to be authentic <sup>46</sup>. The  
433 persuasive evidence in these cases, however, comes from sources other than the sequence  
434 signature.

435         If the BST and other lineage-specific tests based on the single-step codon model are  
436 unreliable in the face of multinucleotide mutation, what should researchers do? The BS+MNM  
437 test could be used to accommodate multinucleotide mutation; our results suggest this may be a  
438 promising approach. But there are many forms of evolutionary complexity that are not  
439 incorporated in this model, such as MNMs that affect three consecutive nucleotides in a codon,  
440 elevated transversion probability within MNMs, and many other kinds of heterogeneity that  
441 might bias the BS+MNM test <sup>47-49</sup>. Other models are also available to incorporate MNMs <sup>9</sup>, but  
442 their accuracy and robustness are not well characterized, either. More work is therefore required  
443 before the BS+MNM or similar models can be used with confidence in the branch-site or similar  
444 tests.

445         A complementary approach is to use functional experiments to explicitly test hypotheses  
446 that specific historical changes in molecular sequence caused changes in function or phenotype  
447 thought to have mediated adaptation <sup>50,51</sup>. Indeed, the bias we observed may help to explain why  
448 some molecular experiments have shown that codons with a high posterior probability of  
449 positive selection in the BST do not contribute to putative adaptive functions, whereas the codon  
450 changes that do confer those functions have low or moderate PPs <sup>52</sup>. Experimental tests provide  
451 the most convincing evidence of a gene's putative adaptive history, but they require time-  
452 consuming laboratory and fieldwork <sup>53,54</sup>, so it is not clear how to implement them on a genome-  
453 wide scale. Future research may develop and validate more robust models to detect positive  
454 selection, and these may help to identify candidate genes for which specific, testable hypotheses

455 of past molecular adaptation on specific phylogenetic lineages can be formulated. The test  
456 primarily used for this purpose till now, however, is unreliable.

457

#### 458 **ACKNOWLEDGEMENTS**

459 We are grateful to the members of the Thornton lab for discussion and helpful comments. We  
460 thank the Beagle2, Midway2, and Tarbell supercomputing clusters at the University of Chicago.  
461 We also thank the developers of HyPhy for presenting an open source platform that allows  
462 limitless customization of standard analyses. Funding was provided by NIH R01GM104397 and  
463 R01GM121931 (JWT), NSF DEB-1601781 (JWT and AV), NSF DBI-1564611 (MWH), and the  
464 Precision Health Initiative of Indiana University (MWH).

465

#### 466 **AUTHOR CONTRIBUTIONS**

467 Analyses were designed by all authors, performed by AV, and interpreted by all authors. The  
468 manuscript was written by AV and JWT with contributions from MWH.

469

#### 470 **COMPETING FINANCIAL INTERESTS**

471 The authors declare no competing financial interests.

472

473



## 474 METHODS

475 **Datasets, quality control, and inference of BST-significant genes.** We analyzed two  
476 previously published comprehensive datasets of protein-coding alignments on a genomic scale,  
477 one in six mammals, the other in six *Drosophila* species (**Supplementary Table 2**)<sup>13,15,45</sup>. We  
478 aimed to apply the branch-site test on every terminal lineage in the *Drosophila* dataset, and on  
479 the human lineage in the mammal dataset. We only retained gene alignments without gross  
480 misalignments, possessing complete coverage in all fly species, and minimally all primate  
481 species. We then applied the branch-site test as implemented in CODEML 4.7 to each alignment,  
482 assuming the phylogenetic relationships reported in the published studies (**Supplementary Fig.**  
483 **2**)<sup>13,15</sup>. Branch lengths and model parameters were estimated for each alignment by maximum  
484 likelihood (ML), and the F3x4 model was used for codon frequencies. We tested each gene in  
485 mammals for selection on the terminal branch leading to humans; in flies, each gene was tested  
486 separately for selection on each of the six terminal branches, and we express the fraction of  
487 positive inferences across genes as the proportion of all tests conducted<sup>6</sup>. As is standard  
488 practice, we calculated P-values using a likelihood ratio test with 1 df ( $\chi^2$ ) which makes the test  
489 conservative under the null hypothesis<sup>6</sup>. Genes were initially identified as having a putative BST  
490 signature of selection at  $P < 0.05$ . We then applied a correction for multiple testing to a false  
491 discovery rate (FDR)  $< 0.20$  using the *q-value* package in R (available at  
492 <http://github.com/jdstorey/qvalue>).

493 To facilitate unambiguous analysis of CMDs, we removed genes containing CMDs  
494 falling in gaps. We also removed genes for which the ML ancestral reconstructions reported by  
495 CODEML at the base of the tested branch differed between the null and positive selection  
496 models, yielding a set of genes with CMDs that do not depend upon which model is chosen. In  
497 flies, 443 gene-tests (“genes”) were retained after these filters and constitute the BST-significant  
498 set of genes from this dataset. No genes on the human lineage were significant after FDR  
499 correction, so we retained as the BST-significant set from this dataset those genes that passed the  
500 ancestral reconstruction filter and had  $P < 0.05$  (**Supplementary Table 2**). The BST-  
501 nonsignificant set of genes comprises all genes that pass the alignment and ancestral  
502 reconstruction filter that are not in the BST-significant set ( $n=6757$ , humans;  $n=6883$ , flies). We  
503 also repeated our analysis of CMD enrichment (see below) using a gene set that had not been  
504 filtered for reconstruction consistency and found that our conclusions were unchanged  
505 (**Supplementary Table 7**).

506 We only considered genes where the ancestral codons (both CMD and non-CMD codons)  
507 have the same reconstruction under the BST null and BST alternate models. In doing so, we have  
508 also excluded CMDs in codons with gaps in the alignment. For example, in the human dataset, of  
509 the 82 genes that initially provided support for positive selection, 30 genes consist of  
510 unambiguously reconstructed codons under the null and alternate model (the BST-significant

511 gene set). In 49 genes, CMDs fall in gaps. We did not consider the ancestral codon  
512 reconstructions at these sites, and excluded these from our analyses due to alignment  
513 ambiguities. The remaining 3 genes have CMDs that do not fall in gaps, for which the ancestral  
514 codons were reconstructed differently under the null and alternate models. If we re-consider  
515 these 3 ‘positively selected’ genes that were excluded, we find 3 additional CMDs, one in each  
516 of the genes. Including these genes made little to no difference to our CMD enrichment results.  
517

518 **Support for positive selection.** CMDs were identified in BST-significant and BST-  
519 nonsignificant genes as codons with 2 or 3 observed nucleotide differences between the ML  
520 states at the ancestral and extant nodes for the branch being tested; non-CMDs are codons with 0  
521 or 1 differences on the branch tested. CMDs were not assessed on branches not tested.

522 To determine the role of CMDs in significant results from the BST, we excluded codon  
523 positions in BST-significant genes containing CMDs, reanalyzed the data using the BST, and  
524 calculated the fraction of tests that retained a significant result ( $P < 0.05$ ).

525 We quantified the proportion of statistical support for positive selection in BST-  
526 significant genes that comes from CMDs as follows. The site-specific support provided by one  
527 codon site in an alignment is the difference between the log-likelihoods of the positive selection  
528 model and the null model given the data at that site. Support for positive selection provided by  
529 all CMDs in a gene ( $support_{CMD}$ ) is the support summed over all CMD sites in the alignment.  
530 The proportion of support provided by CMDs is  $support_{CMD} / (support_{CMD} + support_{nonCMD})$ . This  
531 proportion can be greater than 1 if support by non-CMDs is negative, as occurs if the likelihood  
532 of the null model at non-CMD sites is higher than that of the positive selection model, given the  
533 parameters of each model estimated by ML over all sites.

534 Sites were classified *a posteriori* as under positive selection if their Bayes Empirical  
535 Bayes posterior probability of being in class 2 ( $\omega_2 > 1$ ) under the positive selection model in  
536 CODEML was  $>0.5$  (moderate support) or  $>0.9$  (strong support).

537 We categorized observed CMDs by the minimum number of nonsynonymous single-  
538 nucleotide steps implied under the Goldman-Yang model between the ancestral and derived  
539 states. For each CMD comprising two nucleotide differences, there are two paths by which they  
540 can be interconverted by two single nucleotide steps. We determined whether the steps on these  
541 paths would be nonsynonymous or synonymous using the standard genetic code and then  
542 calculated the mean number of nonsynonymous steps averaged over the two paths. Paths  
543 involving stop-codons were not included. We conducted a similar analysis for all possible  
544 CMDs in the universal genetic code table.  
545

546 **BS+MNM codon substitution**

547 **model and test.** The codon  
548 substitution model of the  
549 classic BST is based on the  
550 Goldman-Yang (GY) model <sup>5</sup>.

$$q_{ij} = \begin{cases} \kappa\pi_j & \text{synonymous transversion} \\ \pi_j & \text{synonymous transition} \\ \kappa\omega\pi_j & \text{non-synonymous transversion} \quad \dots\dots\dots \\ \omega\pi_j & \text{non-synonymous transition} \\ 0 & \text{two or more differences} \end{cases} \quad (1)$$

551 Sequence evolution is modeled as a Markov process, where the matrix element  $q_{ij}$ , the  
552 instantaneous rate of change from ancestral codon  $i$  to derived codon  $j$ , is defined for four types  
553 of changes: synonymous transitions and transversions, and nonsynonymous transitions and  
554 transversions (see  $q_{ij}$  equation 1). Three parameters are estimated from the data by maximum-  
555 likelihood:  $\omega$ , the ratio of nonsynonymous substitution rate to the synonymous substitution rate  
556 ( $d_N/d_S$ );  $\pi_j$ , the equilibrium frequency of codon  $j$ ; and  $\kappa$ , the transversion:transition rate ratio.

557 Element  $q_{ij}$  is zero for substitutions involving more than one difference, so codons with multiple  
558 differences can only evolve through intermediate codons that are a single change away. A  
559 scaling factor applied to the matrix ensures that branch lengths are interpreted as the expected  
560 number of substitutions per codon.

561 We developed a  
562 modification of the GY  
563 model that incorporates  
564 MNMs using the  
565 parameter,  $\delta$ , which  
566 represents the relative  
567 instantaneous rate of double  
568 substitutions to that of  
569 single substitutions (see  $q_{ij}$

$$q_{ij} = \begin{cases} \kappa\pi_j & \text{synonymous transversion} \\ \pi_j & \text{synonymous transition} \\ \kappa\omega\pi_j & \text{non-synonymous transversion} \\ \omega\pi_j & \text{non-synonymous transition} \\ \omega\delta\kappa^2\pi_j & \text{non-synonymous, 2 transversions} \\ \omega\delta\pi_j & \text{non-synonymous, 2 transitions} \quad \dots\dots\dots \\ \omega\delta\kappa\pi_j & \text{non-synonymous, 1 transversion, 1 transition} \\ \delta\pi_j & \text{synonymous, 2 transitions} \\ \delta\kappa^2\pi_j & \text{synonymous, 2 transversions} \\ \delta\kappa\pi_j & \text{synonymous, 1 transversion, 1 transition} \\ 0 & \text{otherwise} \end{cases} \quad (2)$$

570 equation 2). When  $\delta = 0$ , the BS+MNM model reduces to the classic BST model that does not  
571 incorporate MNMs ( $q_{ij}$  equation 1). Triple substitutions have an instantaneous rate of zero.

572 The BS+MNM test of positive selection is identical to the BST, except it utilizes this  
573 MNM codon model. We implemented this test by modifying the branch-site test batch file  
574 (YangNielsenBranchSite2005.bf) in Hyphy 2.2.6 software by declaring  $\delta$  a global variable,  
575 incorporating it into the codon table, and allowing it to be optimized by ML as it other model  
576 parameters are.

577 We validated the BS+MNM implementation by simulating 50 replicate alignments using  
578 the BS+MNM null model in Hyphy under genome-median parameters (see below). We then  
579 used the BS+MNM procedure to find the ML estimate of each parameter, including branch  
580 lengths, given each alignment and the topology of the phylogeny used to generate the sequences.  
581 We compared the distribution of estimates over replicates to the “true” values used to generate  
582 the sequences (**Supplementary Fig. 3**).

583 To test if there is statistical support in the data for the BS+MNM null model relative to  
584 the standard BST null model, we performed an LRT with 1 df, comparing the fit of the  
585 BS+MNM null model and the BST null model on our empirical genes. Briefly, for each of the  
586 6868 human genes, we tested if the BS+MNM null model fit the data better than the BST null  
587 model at  $P < 0.05$  and also applied an adjustment for multiple testing ( $FDR < 0.2$ ). We performed  
588 similar LRTs for each of the six terminal lineages in flies. To determine whether this test might  
589 be prone to falsely infer support for the BS+MNM model, we simulated control sequences under  
590 the null BST model with parameters derived from the empirical sequences and performed the  
591 LRT as described above. Only 2 percent of genes in humans and 2.6 percent in flies yielded  
592 significant support for BS+MNM at  $P < 0.05$ . Zero human genes and 0.006 percent of fly genes  
593 retained significance after multiple testing adjustment ( $FDR < 0.2$ ). (**Supplementary Table 4**).

594  
595

596 **Simulations and analysis of false-positive bias.** To characterize bias in the BST and other tests  
597 of selection, we conducted sequence simulations in the absence of positive selection under  
598 empirically derived conditions. We used the BS+MNM method we implemented in Hyphy to  
599 estimate by maximum likelihood (ML) the gene-specific branch lengths and parameters of the  
600 null BS+MNM model for every gene in the mammalian and fly datasets. We also calculated the  
601 genome-wide median of each parameter over all genes in each dataset (the “genome-average”  
602 parameter value). Probability density characterizations for parameters  $\delta$  and gene length were  
603 performed using the *density* function in R.

604 We simulated sequence evolution under the BS+MNM null model using either gene-  
605 specific or genome-median parameters. First, we simulated a “pseudo-genome” without positive  
606 selection by simulating one replicate of each of the 6868 and 8564 mammalian and fly  
607 alignment, each at its empirical length, using the BS+MNM null model and the ML parameter  
608 estimates inferred for that gene from the empirical data. We then ran the BST on these  
609 sequences, testing for signatures of positive selection on the human lineage and each terminal fly  
610 lineage (**Supplementary Table 2**). Control simulations were conducted under identical  
611 conditions but with  $\delta = 0$ .

612 To test the effect of gene length on bias in the BST, we focused on genes in the BST-  
613 significant set. For each gene’s gene-specific parameters, we simulated 50 replicates alignments  
614 of length 5,000 or 10,000 codons. We analyzed these alignments using the BST, assigning the  
615 human branch as foreground for mammalian genes or, for flies, the same branch that produced a  
616 significant result when the empirical data were analyzed. The false positive rate (FPR) for any  
617 gene’s parameters is the fraction of replicates yielding a positive test ( $P < 0.05$ ). We also repeated  
618 these simulations and analyses using the genome-median value of  $\delta$ . For control experiments  
619 without MNMs, we set  $\delta = 0$  in the simulations.

620 To test the effect of the rate at which MNM substitutions are produced on false positive  
621 inference rates, we simulated evolution of alignments 5,000 codons long under the BS+MNM  
622 null model, using genome-median estimates for all parameters except  $\delta$ , which we varied. At  
623 each value of  $\delta$ , we simulated 50 replicates. We analyzed each replicate using the BST for  
624 selection on the human or *D. simulans* lineages and calculated the proportion of replicates for  
625 each value of  $\delta$  that yielded a false positive inference ( $P < 0.05$ ).

626 We computed the observed proportion of tandem substitutions as a fraction of all  
627 substitutions on the human and *D. melanogaster* lineages in both empirical and simulated  
628 datasets. For each of the 6868 genes in the curated mammalian dataset, we aligned the human  
629 gene to the inferred sequence of the human-chimp ancestor, identified all substitutions as  
630 differences between these sequences, and calculated the proportion of tandem substitutions,  $T$ , as  
631 the number of substitutions at adjacent sites divided by the sum of substitutions at adjacent sites  
632 and those at non-adjacent sites across all sites in the dataset. Differences at adjacent sites were  
633 counted as a single tandem substitution. For each of the 8564 genes in the fly dataset, we aligned  
634 the *D. melanogaster* sequence to the *D. melanogaster/D. simulans* ancestor and followed the  
635 procedure described above. For simulated sequences, we repeated this procedure using the  
636 sequences simulated under the BS+MNM null model and parameters estimated from each gene  
637 in the empirical datasets.

638

639 **BUSTED.** To examine the accuracy of BUSTED, we used Hyphy software 2.2.6 (batch files  
640 BUSTED.bf and QuickSelectionDetection.bf). We analyzed the 5,000 codon-long alignments  
641 simulated under the BS+MNM null model, using parameters estimated by ML for each BST-  
642 significant gene, with  $\delta$  assigned either to its gene-specific estimate, its genome-average, or to  
643 zero. We applied BUSTED to the replicate alignments to test for selection ( $P < 0.05$ ) on the  
644 human lineage or the same fly lineage that was significant for that gene in the BST of the  
645 empirical data.

646

647 **Power analyses.** To characterize the statistical power of the BST and BS+MNM tests, we  
648 simulated sequence evolution with positive selection of variable intensity and pervasiveness  
649 (**Supplementary Fig. 4**). Specifically, we used the BS positive model in Hyphy to simulate  
650 sequence evolution with the human and *D. simulans* terminal branches as the foreground  
651 branches. We used genome-average estimates of all parameters, including gene length (418 and  
652 510 codons for mammals and flies, respectively), but we varied  $\omega_2$  and  $p_2$ . 20 replicate  
653 alignments were simulated under each set of conditions and then analyzed using the BST, the  
654 BS+MNM test, or BUSTED. For each set of conditions, the true positive rate was calculated as  
655 the fraction of replicates yielding a significant test of positive selection ( $P < 0.05$  for BST and  
656 BS+MNM,  $FDR < 0.20$  for at least one site in the alignment for BUSTED).

657

658 **BS+MNM+  $\kappa_2$  model:**

659 We developed the  
660 BS+MNM+  $\kappa_2$  model,  
661 which incorporates into  
662 the BS+MNM model ( $q_{ij}$   
663 equation 2) two different  
664 transversion:transition  
665 rate ratio parameters,  $\kappa_1$

$$q_{ij} = \begin{cases} \kappa_1 \pi_j & \text{synonymous transversion} \\ \pi_j & \text{synonymous transition} \\ \omega \kappa_1 \pi_j & \text{non-synonymous transversion} \\ \omega \pi_j & \text{non-synonymous transition} \\ \omega \delta \kappa_2^2 \pi_j & \text{non-synonymous, 2 transversions} \\ \omega \delta \pi_j & \text{non-synonymous, 2 transitions} \\ \omega \delta \kappa_2 \pi_j & \text{non-synonymous, 1 transversion, 1 transition} \quad \dots\dots\dots (3) \\ \delta \pi_j & \text{synonymous, 2 transitions} \\ \delta \kappa_2^2 \pi_j & \text{synonymous, 2 transversions} \\ \delta \kappa_2 \pi_j & \text{synonymous, 1 transversion, 1 transition} \\ 0 & \text{otherwise} \end{cases}$$

666 for single-site substitutions and  $\kappa_2$  for MNMs (see  $q_{ij}$  equation 3). All free parameters of the  
667 model are estimated by ML given a sequence alignment. This model was implemented by  
668 further modifying our BS+MNM batchfile in Hyphy 2.2.6 software by declaring  $\kappa_2$  a global  
669 variable, incorporating it into the codon table, and allowing it to be optimized by ML as other  
670 parameters are in the batch file.

671 For validation, we estimated the parameters of the BS+MNM+  $\kappa_2$  null model by ML for  
672 every alignment in each dataset and calculated the genome-average median estimate of each  
673 parameter (Fig. S7). We then simulated 50 replicate alignments of length 418 and 510 codons in  
674 the mammalian and fly datasets respectively, under the BS+MNM+  $\kappa_2$  null model with all model  
675 parameters set to their genome-wide median. We then estimated each parameter by ML under  
676 the null model given each alignment and compared the distribution of estimates to the parameters  
677 used to generate the alignments. We found that most parameters were estimated accurately, but  
678 estimates of  $\kappa_2$  had high variance (**Supplementary Fig. S7**), presumably because the quantity of  
679 data in a single gene, in which CMDs are typically rare, is inadequate to support a robust  
680 estimate of this parameter. We therefore limited our use of this model to generating sequences  
681 by simulation rather than making inferences from sequence data.

682 To determine the effect of the MNM-specific transversion:transition rate on false-positive  
683 bias in the BST, we simulated sequences 10,000 codons long under the BS+MNM+ $\kappa_2$  null  
684 model, using genome-median parameters except  $\kappa_2$ , which we varied. For each value of  $\kappa_2$ , we  
685 simulated 50 replicates, applied the BST, and calculated the FPR as the fraction of replicates  
686 yielding a positive inference ( $P < 0.05$ ).  
687

688 **Data availability.** The empirical alignments reanalyzed in this study are available in the  
689 supplementary information of the original publications that generated these data <sup>12, 16, 45</sup>.  
690

691 **Code availability.** The custom HYPHY batch codes for the BS+MNM and BS+MNM+ $\kappa_2$  tests  
692 are available as supplementary files and at  
693 [https://github.com/JoeThorntonLab/MNM\\_SelectionTests](https://github.com/JoeThorntonLab/MNM_SelectionTests).  
694

695

696 **REFERENCES**

697

- 698 1. Goldman, N. & Yang, Z. A codon-based model of nucleotide substitution for protein-  
699 coding DNA sequences. *Mol Biol Evol* **11**, 725-736 (1994).
- 700 2. Murrell, B. et al. Gene-wide identification of episodic selection. *Mol Biol Evol* **32**, 1365-  
701 1371 (2015).
- 702 3. Murrell, B. et al. Detecting individual sites subject to episodic diversifying selection. *PLoS*  
703 *Genet* **8**, e1002764 (2012).
- 704 4. Smith, M. D. et al. Less is more: an adaptive branch-site random effects model for efficient  
705 detection of episodic diversifying selection. *Mol Biol Evol* **32**, 1342-1353 (2015).
- 706 5. Yang, Z. & Nielsen, R. Codon-substitution models for detecting molecular adaptation at  
707 individual sites along specific lineages. *Mol Biol Evol* **19**, 908-917 (2002).
- 708 6. Zhang, J., Nielsen, R. & Yang, Z. Evaluation of an improved branch-site likelihood method  
709 for detecting positive selection at the molecular level. *Mol Biol Evol* **22**, 2472-2479 (2005).
- 710 7. Pond, S. L., Frost, S. D. & Muse, S. V. HyPhy: hypothesis testing using phylogenies.  
711 *Bioinformatics* **21**, 676-679 (2005).
- 712 8. Kosiol, C., Holmes, I. & Goldman, N. An empirical codon model for protein sequence  
713 evolution. *Mol Biol Evol* **24**, 1464-1479 (2007).
- 714 9. Whelan, S. & Goldman, N. Estimating the frequency of events that cause multiple-  
715 nucleotide changes. *Genetics* **167**, 2027-2043 (2004).
- 716 10. Muse, S. V. & Gaut, B. S. A likelihood approach for comparing synonymous and  
717 nonsynonymous nucleotide substitution rates, with application to the chloroplast genome.  
718 *Mol Biol Evol* **11**, 715-724 (1994).
- 719 11. Yang, Z. & dos Reis, M. Statistical properties of the branch-site test of positive selection.  
720 *Mol Biol Evol* **28**, 1217-1228 (2011).
- 721 12. Han, M. V., Demuth, J. P., McGrath, C. L., Casola, C. & Hahn, M. W. Adaptive evolution  
722 of young gene duplicates in mammals. *Genome Res* **19**, 859-867 (2009).
- 723 13. Drosophila, G. C. et al. Evolution of genes and genomes on the Drosophila phylogeny.  
724 *Nature* **450**, 203-218 (2007).
- 725 14. Foote, A. D. et al. Convergent evolution of the genomes of marine mammals. *Nat Genet*  
726 **47**, 272-275 (2015).
- 727 15. Kosiol, C. et al. Patterns of positive selection in six Mammalian genomes. *PLoS Genet* **4**,  
728 e1000144 (2008).
- 729 16. Roux, J. et al. Patterns of positive selection in seven ant genomes. *Mol Biol Evol* **31**, 1661-  
730 1685 (2014).
- 731 17. Zhang, J. Performance of likelihood ratio tests of evolutionary hypotheses under inadequate  
732 substitution models. *Mol Biol Evol* **16**, 868-875 (1999).
- 733 18. Nozawa, M., Suzuki, Y. & Nei, M. Reliabilities of identifying positive selection by the  
734 branch-site and the site-prediction methods. *Proc Natl Acad Sci U S A* **106**, 6700-6705  
735 (2009).
- 736 19. Casola, C. & Hahn, M. W. Gene conversion among paralogs results in moderate false  
737 detection of positive selection using likelihood methods. *J Mol Evol* **68**, 679-687 (2009).
- 738 20. Anisimova, M. & Yang, Z. Multiple hypothesis testing to detect lineages under positive  
739 selection that affects only a few sites. *Mol Biol Evol* **24**, 1219-1228 (2007).

- 740 21. Kosakovsky Pond, S. L. et al. A random effects branch-site model for detecting episodic  
741 diversifying selection. *Mol Biol Evol* **28**, 3033-3043 (2011).
- 742 22. Zhang, J. Frequent false detection of positive selection by the likelihood method with  
743 branch-site models. *Mol Biol Evol* **21**, 1332-1339 (2004).
- 744 23. Gharib, W. H. & Robinson-Rechavi, M. The branch-site test of positive selection is  
745 surprisingly robust but lacks power under synonymous substitution saturation and variation  
746 in GC. *Mol Biol Evol* **30**, 1675-1686 (2013).
- 747 24. Zhai, W., Nielsen, R., Goldman, N. & Yang, Z. Looking for Darwin in genomic sequences-  
748 -validity and success of statistical methods. *Mol Biol Evol* **29**, 2889-2893 (2012).
- 749 25. Schrider, D. R., Hourmozdi, J. N. & Hahn, M. W. Pervasive multinucleotide mutational  
750 events in eukaryotes. *Curr Biol* **21**, 1051-1054 (2011).
- 751 26. Saribasak, H. et al. DNA polymerase  $\zeta$  generates tandem mutations in immunoglobulin  
752 variable regions. *J Exp Med* **209**, 1075-1081 (2012).
- 753 27. Loeb, L. A. & Monnat, R. J. DNA polymerases and human disease. *Nat Rev Genet* **9**, 594-  
754 604 (2008).
- 755 28. Matsuda, T., Bebenek, K., Masutani, C., Hanaoka, F. & Kunkel, T. A. Low fidelity DNA  
756 synthesis by human DNA polymerase-eta. *Nature* **404**, 1011-1013 (2000).
- 757 29. Seplyarskiy, V. B., Bazykin, G. A. & Soldatov, R. A. Polymerase  $\zeta$  Activity Is Linked to  
758 Replication Timing in Humans: Evidence from Mutational Signatures. *Mol Biol Evol* **32**,  
759 3158-3172 (2015).
- 760 30. Stone, J. E., Lujan, S. A., Kunkel, T. A. & Kunkel, T. A. DNA polymerase zeta generates  
761 clustered mutations during bypass of endogenous DNA lesions in *Saccharomyces*  
762 *cerevisiae*. *Environ Mol Mutagen* **53**, 777-786 (2012).
- 763 31. Arana, M. E., Seki, M., Wood, R. D., Rogozin, I. B. & Kunkel, T. A. Low-fidelity DNA  
764 synthesis by human DNA polymerase theta. *Nucleic Acids Res* **36**, 3847-3856 (2008).
- 765 32. Besenbacher, S. et al. Multi-nucleotide de novo Mutations in Humans. *PLoS Genet* **12**,  
766 e1006315 (2016).
- 767 33. Chen, J. M., Férec, C. & Cooper, D. N. Complex Multiple-Nucleotide Substitution  
768 Mutations Causing Human Inherited Disease Reveal Novel Insights into the Action of  
769 Translesion Synthesis DNA Polymerases. *Hum Mutat* **36**, 1034-1038 (2015).
- 770 34. Chen, J. M., Cooper, D. N. & Férec, C. A new and more accurate estimate of the rate of  
771 concurrent tandem-base substitution mutations in the human germline: ~0.4% of the single-  
772 nucleotide substitution mutation rate. *Hum Mutat* **35**, 392-394 (2014).
- 773 35. Harris, K. & Nielsen, R. Error-prone polymerase activity causes multinucleotide mutations  
774 in humans. *Genome Res* **24**, 1445-1454 (2014).
- 775 36. Hodgkinson, A. & Eyre-Walker, A. Variation in the mutation rate across mammalian  
776 genomes. *Nat Rev Genet* **12**, 756-766 (2011).
- 777 37. Francioli, L. C. et al. Genome-wide patterns and properties of de novo mutations in  
778 humans. *Nat Genet* **47**, 822-826 (2015).
- 779 38. Assaf, Z. J., Tilk, S., Park, J., Siegal, M. L. & Petrov, D. A. Deep sequencing of natural and  
780 experimental populations of *Drosophila melanogaster* reveals biases in the spectrum of new  
781 mutations. *Genome Res* **27**, 1988-2000 (2017).
- 782 39. Zhu, W. et al. Concurrent nucleotide substitution mutations in the human genome are  
783 characterized by a significantly decreased transition/transversion ratio. *Hum Mutat* **36**, 333-  
784 341 (2015).
- 785 40. Averof, M., Rokas, A., Wolfe, K. H. & Sharp, P. M. Evidence for a high frequency of

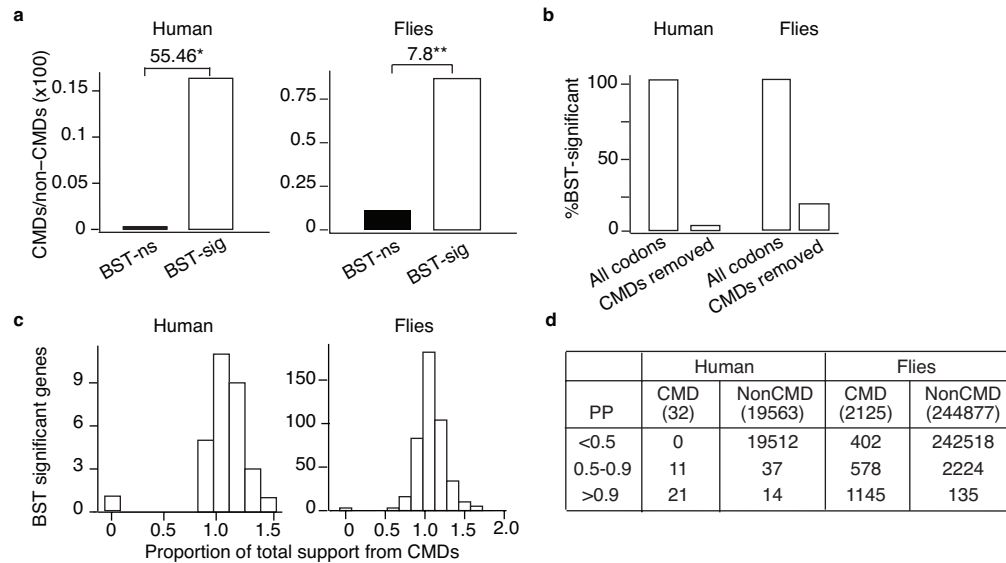


- 786 simultaneous double-nucleotide substitutions. *Science* **287**, 1283-1286 (2000).
- 787 41. Bazykin, G. A., Kondrashov, F. A., Ogurtsov, A. Y., Sunyaev, S. & Kondrashov, A. S.  
788 Positive selection at sites of multiple amino acid replacements since rat-mouse divergence.  
789 *Nature* **429**, 558-562 (2004).
- 790 42. Rogozin, I. B. et al. Evolutionary switches between two serine codon sets are driven by  
791 selection. *Proc Natl Acad Sci U S A* **113**, 13109-13113 (2016).
- 792 43. Suzuki, Y. False-positive results obtained from the branch-site test of positive selection.  
793 *Genes Genet Syst* **83**, 331-338 (2008).
- 794 44. De Maio, N., Holmes, I., Schlötterer, C. & Kosiol, C. Estimating empirical codon hidden  
795 Markov models. *Mol Biol Evol* **30**, 725-736 (2013).
- 796 45. Larracuenta, A. M. et al. Evolution of protein-coding genes in *Drosophila*. *Trends Genet*  
797 **24**, 114-123 (2008).
- 798 46. Sironi, M., Cagliani, R., Forni, D. & Clerici, M. Evolutionary insights into host-pathogen  
799 interactions from mammalian sequence data. *Nat Rev Genet* **16**, 224-236 (2015).
- 800 47. Bloom, J. D. An experimentally determined evolutionary model dramatically improves  
801 phylogenetic fit. *Mol Biol Evol* **31**, 1956-1978 (2014).
- 802 48. Lopez, P., Casane, D. & Philippe, H. Heterotachy, an important process of protein  
803 evolution. *Mol Biol Evol* **19**, 1-7 (2002).
- 804 49. Pond, S. K. & Muse, S. V. Site-to-site variation of synonymous substitution rates. *Mol Biol*  
805 *Evol* **22**, 2375-2385 (2005).
- 806 50. Barber, M. F. & Elde, N. C. Nutritional immunity. Escape from bacterial iron piracy  
807 through rapid evolution of transferrin. *Science* **346**, 1362-1366 (2014).
- 808 51. Chan, Y. F. et al. Adaptive evolution of pelvic reduction in sticklebacks by recurrent  
809 deletion of a *Pitx1* enhancer. *Science* **327**, 302-305 (2010).
- 810 52. Field, S. F., Bulina, M. Y., Kelmanson, I. V., Bielawski, J. P. & Matz, M. V. Adaptive  
811 evolution of multicolored fluorescent proteins in reef-building corals. *J Mol Evol* **62**, 332-  
812 339 (2006).
- 813 53. Barrett, R. D. & Hoekstra, H. E. Molecular spandrels: tests of adaptation at the genetic  
814 level. *Nat Rev Genet* **12**, 767-780 (2011).
- 815 54. Siddiq, M.A, Loehlin, D.W., Montooth, K.L., Thornton J.W. Experimental test and  
816 refutation of a classic case of molecular adaptation in *Drosophila melanogaster*. *Nature*  
817 *Ecology and Evolution* 1, doi:10.1038/s41559-016-0025 (2017)

818

819

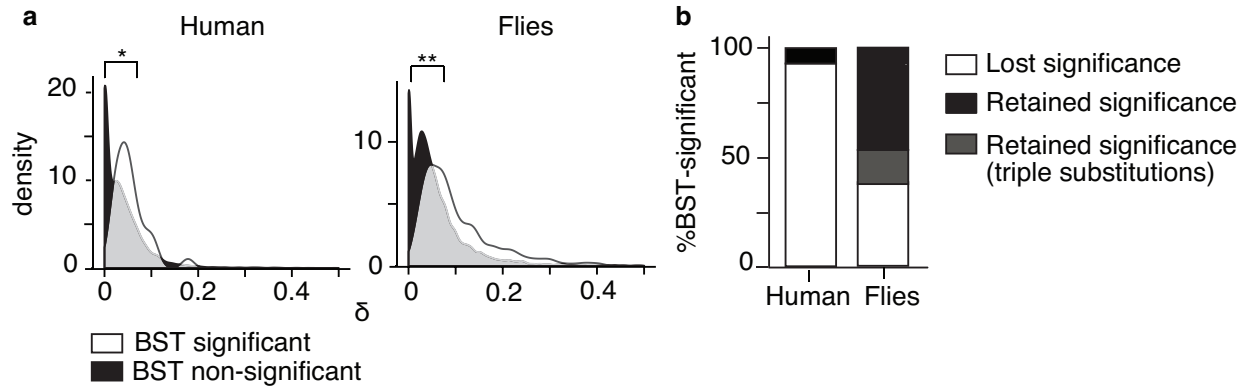
820



821  
822  
823  
824  
825  
826  
827  
828  
829  
830  
831  
832  
833  
834  
835  
836  
837  
838  
839  
840  
841

**Figure 1** Codons with multiple nucleotide differences (CMDs) drive branch-site signatures of selection.

- (a) CMDs are enriched in genes with a signature of positive selection. Codons were classified by the number of nucleotide differences between the ancestral and terminal states on branches tested for positive selection. CMDs have  $\geq 2$  differences; non-CMDs have  $\leq 1$  difference. The CMD/non-CMD ratio is shown for genes with a significant signature of selection in the BST (BST-sig) and those without (BST-ns). Fold-enrichment is shown as the odds ratio. \*,  $P=4e-4$  by  $\chi^2$  test; \*\*,  $P=1e-41$  by Fisher's exact test.
- (b) Percentage of genes that retain a signature of positive selection when CMDs are excluded from the branch-site test analysis.
- (c) Distribution across BST-significant genes of the proportion of total support for the positive selection model that is provided by CMDs. Total support is the difference in log-likelihood between the positive selection and null models, summed over all codons in the alignment. Support from CMDs is summed over codons with multiple differences. The proportion of support from CMDs can be greater than 1 if the log-likelihood difference between models is negative at non-CMDs.
- (d) Most codons classified as positively selected are CMDs. The number of CMDs and non-CMDs in BST-significant genes are shown according to their Bayes Empirical Bayes posterior probability (PP) of being in the positively selected class.



842

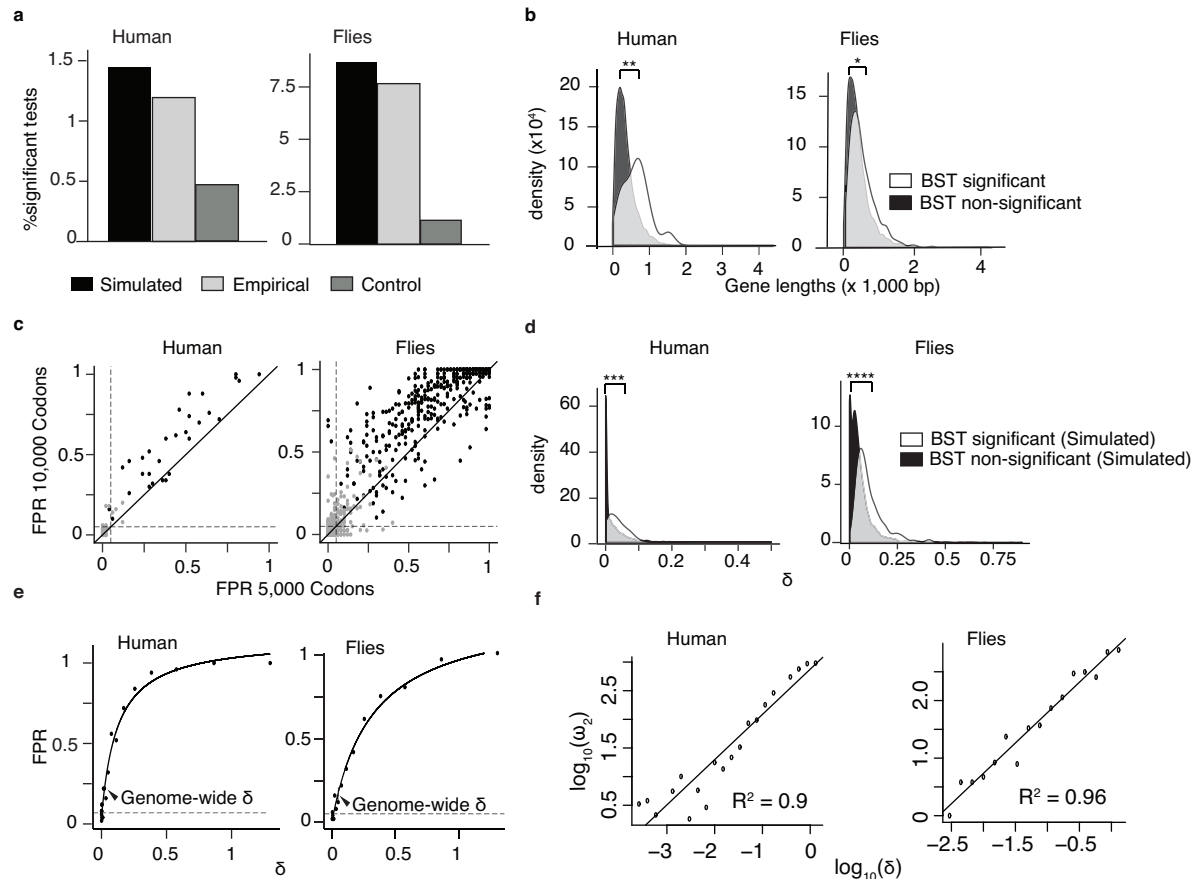
843

844

845 **Figure 2** Incorporating MNMs into the branch-site model eliminates the signature of positive  
846 selection in many genes. The mammalian and fly datasets were reanalyzed using a version of the  
847 BST that allows MNMs (BS+MNM) by including a parameter  $\delta$ , a multiplier on the rate of each  
848 double substitution relative to single substitutions.

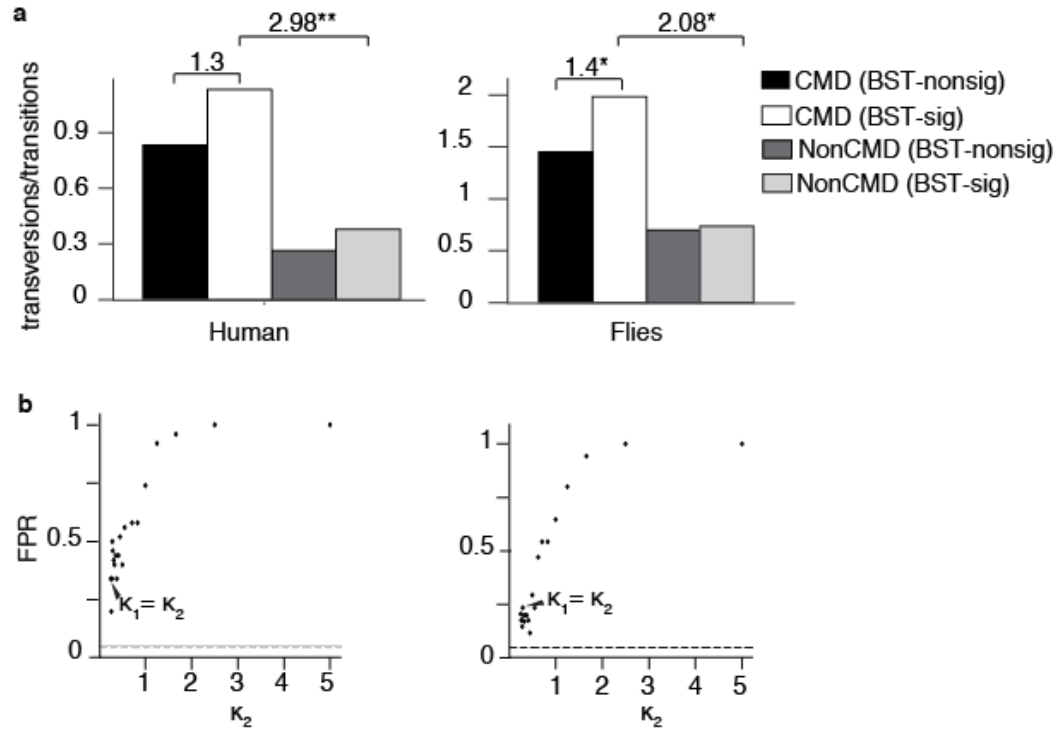
849 (a) The distribution of ML estimates of  $\delta$  across genes with (white) and without (black) a  
850 significant result in the classic BST is shown for empirical alignments. Median estimates of  $\delta$   
851 in BST-significant and BST-nonsignificant genes are 0.047 and 0.026 in humans,  
852 respectively, and 0.107 and 0.062 in flies. \*,  $P=6.7e-4$ ; \*\*,  $P=1e-8$  by Mann-Whitney U  
853 Test.

854 (b) Proportion of genes with a significant result in the BST that lose or retain that signature using  
855 the BS+MNM test. Genes that remain significant but contain CMDs with three differences,  
856 which are not incorporated into BS+MNM, are also shown.



857  
 858 **Figure 3** MNMs cause a strong bias in the branch-site test under realistic conditions. For each  
 859 gene in the mammalian and fly datasets, the parameters of the BS+MNM null model were  
 860 estimated by maximum likelihood. We then simulated sequence evolution under each gene's  
 861 inferred null parameters and used the classic BST on the simulated alignments to test for positive  
 862 selection on the human and terminal fly lineages.  
 863 (a) The fraction of all tests that are BST-significant ( $P < 0.05$ ) is shown for the data simulated  
 864 under the BS+MNM null model, the original empirical sequence alignments, and a control  
 865 dataset simulated with  $\delta = 0$ . Each gene's length in the simulation was identical to its  
 866 empirical length.  
 867 (b) BST-significant genes are longer than BST non-significant genes. The probability density of  
 868 gene lengths in the two categories is shown for the empirical mammalian and fly datasets.  
 869 Median lengths in BS-significant and non-significant genes, respectively, were 642 and 343  
 870 bp in humans; in flies, 448 and 399 bp. The difference between the two distributions was  
 871 evaluated using a Mann-Whitney U test. \*,  $P = 8e-4$ ; \*\*,  $P = 8e-5$ ;  
 872 (c) Systematic bias in the BST. For each gene with a significant result in the BST using the  
 873 empirical data, we simulated 50 replicates using the BS+MNM null model and the ML  
 874 parameter estimates for that gene at lengths of 5,000 and 10,000 codons; these data were then  
 875 analyzed using the BST. The false positive rate (FPR) for any gene's simulation (black  
 876 points) is the proportion of replicates with  $P < 0.05$ . Gray points show FPR for control  
 877 simulations with  $\delta = 0$ . Dashed lines, FPR of 0.05. The solid diagonal line has a slope of 1.  
 878 (d) The distribution of ML estimates of  $\delta$  across genes with (white) and without (black) a  
 879 signature of positive selection in the classic BST is shown for data simulated under the

880 BS+MNM null model. Median  $\delta$  in BST-significant and BST-nonsignificant genes = 0.03  
881 and 0.0009 in humans, 0.04 and 0.08 in flies. Difference between the distributions was  
882 evaluated using a Mann-Whitney U Test. \*\*\*,  $P=1e-12$ ; \*\*\*\*,  $P=1e-199$ .  
883 **(e)** Increasing the MNM rate increases bias in the BST. Sequences 5,000 codons long were  
884 simulated using the BS+MNM model and the median value of each model parameter and  
885 branch length across all genes in each dataset, but  $\delta$  was allowed to vary. The rate of false  
886 positives ( $P<0.05$ ) in 50 replicates at each value of  $\delta$  is shown. Solid line, hyperbolic fit to  
887 the data; dotted line, FPR level of 5%. Arrowhead, median  $\delta$  across all genes.  
888 **(f)** Relationship between  $\delta$  and inferred  $\omega_2$ . Sequences simulated in (e) were used to infer  
889 the  $\omega_2$  estimated by BST under the positive selection model, and the relationship  
890 plotted on a log-log scale. The best-fit linear regression line is shown along with the  
891 coefficient of determination.  
892  
893

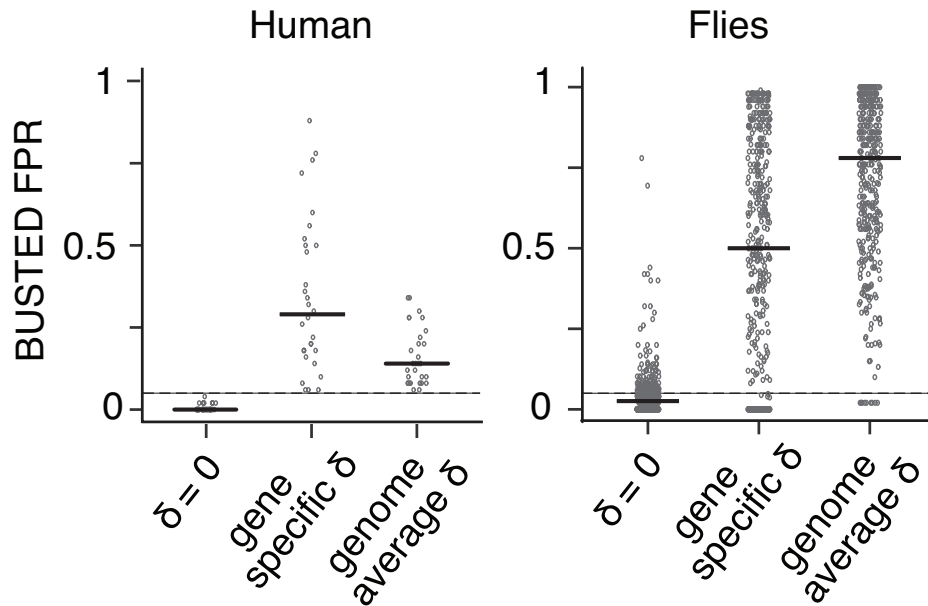


894  
895  
896  
897  
898  
899  
900  
901  
902  
903  
904  
905  
906  
907

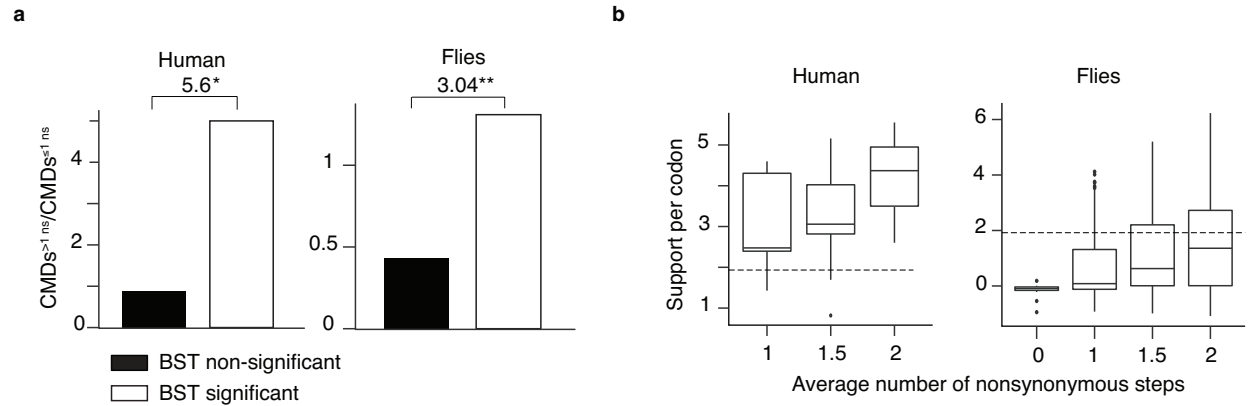
**Figure 4** Transversion-enrichment in CMDs biases the BST.

**(a)** The ratio of transversions:transitions observed in CMDs and in non-CMDs is shown for BST-significant and BST-nonsignificant genes. Fold-enrichment is shown as the odds ratio. \*,  $P=5e-4$ ; \*\*,  $P=3e-25$  by Fisher's exact test.

**(b)** Increasing the transversion rate in MNMs increases bias of the BST. Sequences 10,000 codons long were simulated using an elaboration of the BS+MNM model that allows MNMs to have a transversion:transition rate ( $\kappa_2$ ) different from that in single-nucleotide substitutions ( $\kappa_1$ ). 50 replicate alignments were simulated under the null model using the average value of every model parameter and branch length across all genes in each dataset, except  $\kappa_2$  was allowed to vary. The rate of false positives ( $P<0.05$ ) at each value of  $\kappa_2$  is shown. Arrowheads show the false positive rate when sequences were simulated with  $\kappa_2$  equal to  $\kappa_1$ . Dotted line, FPR of 5%.



908  
909 **Figure 5** MNMs bias a newer test of positive selection. False positive inferences under realistic  
910 conditions using BUSTED. For every BST-significant gene in each dataset, 50 replicate  
911 alignments 5,000 codons long were simulated using the BS+MNM null model and parameter  
912 values estimated from the empirical sequences. These alignments were then analyzed for a  
913 signature of positive selection ( $P < 0.05$ ) using BUSTED.  $\delta$  was assigned to its gene-specific  
914 estimate, to its average across all genes in each dataset, or to zero. FPR is the proportion of  
915 replicate alignments for each gene with  $P < 0.05$ . Each dot represents the FPR for one gene; black  
916 bars are the median across genes.  
917  
918



919  
920  
921  
922  
923  
924  
925  
926  
927  
928  
929  
930  
931  
932  
933  
934

**Figure 6** CMDs implying multiple nonsynonymous steps drive the BST.

- (a) For every CMD, the mean of the number of nonsynonymous single-nucleotide steps on the two direct paths between the ancestral and derived states was calculated. In BST-significant and BST-nonsignificant genes, the ratio of CMDs invoking more than one nonsynonymous step to those invoking one or fewer such steps is shown. Fold-enrichment is shown as the odds ratio. \*,  $P=9e-04$ ; \*\* $P= 1.6e-67$  by Fisher's exact test.
- (b) Support for the positive selection model provided by CMDs depends on the number of implied nonsynonymous single-nucleotide steps. Support is the log-likelihood difference between the positive selection and null models of the BST given the data at a single codon site. Box plots show the distribution of support by CMDs in BST significant genes categorized according to the mean number of implied nonsynonymous steps. Dotted line, support of 1.92, at which the BST yields a significant result for an entire gene ( $P<0.05$ ). In human BST-significant genes, no CMDs imply zero non-synonymous changes.